AT&T Technical Journal
Vol. 64, No. 4, April 1985
Printed in U.S.A.

# A Controlled Impedance Robot Gripper

By M. K. BROWN*

(Manuscript received June 5, 1984)

The design of robot grippers has traditionally involved pneumatics or gear reduction electric drives that do not allow for the control of the stiffness of the mechanism. The manipulation of fragile objects such as eggs or light bulbs requires the gripper to be able to close on the object with minimal impact forces, and yet maintain a static grip force sufficient to firmly handle the object. This paper describes a two-fingered controlled impedance gripper where the impedance is imparted by electrical means. The analog control system allows independent control of the effective mechanical mass and damping of each finger, as well as additional control of common-mode versus differential-mode response. The gripper is modeled by a computer simulation that consists of a set of nonlinear differential equations with time-varying feedback parameters. In the final form the model has ten degrees of mechanical freedom and eight electrical poles, i.e., an 18th-order nonlinear differential equation. The dynamic equations are described and results given are compared with actual results obtained from laboratory experiments with the gripper. An Appendix describes the method of solution used for the nonlinear differential equations. The accuracy of the simulation has been verified by measurements on the actual gripper. This analysis has resulted in the design of a gripper control system capable of providing controlled compliance and reduced finger impact forces while maintaining a quick response and firm grasp.

## I. INTRODUCTION

Many compliant mechanisms have been built using mechanical means for obtaining the compliant properties. For example, the Remote Center Compliant manipulator (RCC), developed by Whitney

* AT&T Bell Laboratories.

and Nevins[1] at Draper Labs, utilizes specially designed springs in a configuration that allows free angular movement about a radial center while maintaining high stiffness along the radius. This device is particularly useful for inserting a pin in a hole or for analogous tasks, but the amount of compliance is fixed while in operation.

Similar devices have been developed by the Lord Corporation and others. One interesting device was designed by M. Cutkowski.[2] It replaces the fixed springs of the RCC device with fluid-filled elastomer bubbles. The compliance thus formed is nonlinear and adjustable by changing the fluid pressure. This feature makes the compliant wrist a potentially active device with bandwidth limited only by the rapidity with which fluid pressure may be changed.

Another compliant manipulator was designed by Hanafusa and Asada, who developed a three-fingered gripper with spring-driven fingers.[3] The fingers are arranged in a circle and have rollers on the fingertips. Much of their work has involved determining stable gripping orientations for irregularly shaped objects.

Dynamic computer control of the amount of compliance and damping imparted to the gripper is desirable since this allows the gripper to adapt to various grasping tasks as they proceed without the need to exchange mechanical parts such as springs.[4] For a two-fingered gripper, a "common-mode" compliance and "differential-mode" compliance can be made usefully different so that a gripper may use a delicate grasp and still hold an object firmly in place.

Figure 1 illustrates the construction of the two-fingered gripper. The fingers are mounted on linear bearing slides and driven through a rack and pinion by two dc servomotors. The two fingers are driven independently by two dc servomotors. Thus, the gripper can close from either side and need not be centered on an object before closing.

A particularly important feature of this mechanical design is the rack and pinion servomotor device. This mechanism is mechanically back drivable, meaning that a force applied to the finger will cause the motor to move. A typical worm drive mechanism, for example, would not have this characteristic because of high internal friction. This feature allows the motor drive mechanism to function as a mechanical impedance (under computer control) applying all of the appropriate effects of mass, damping, and compliance directly to the fingers.

To control the position of the gripper fingers, a means of measuring their positions is necessary. A capacitive measuring system was developed (see Ref. 5) that has the properties of low noise (s/n $>$ 90 dB), low mass, and fast transient response. It consists of a metal rod sliding inside an insulated metal tube. The capacitance of the rod and tube varies as a function of the position of the finger. A capacitance measurement circuit produces a voltage proportional to

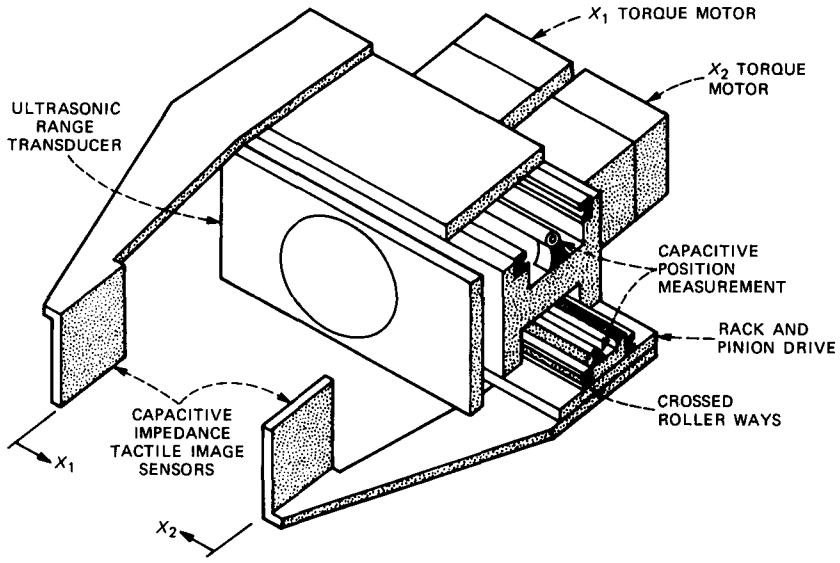


Fig. 1—Instrumented controlled impedance gripper.

the capacitance. The position measurement error developed by this system is less than 1 percent, while the step response rise time is about 150 $\mu$s.

The dc servomotor performance can be modeled by an electrical and mechanical system consisting of an armature resistance and inductance, a back Electromotive Force (EMF), armature inertia, and bearing friction. This forms a third-order differential equation describing the current-voltage relationship as well as the torque output of the motor. Since torque is a quantity that must be controlled and torque is an essentially linear function of motor current, it is desirable to drive the motor with a current source. This reduces the motor equations to second order and greatly simplifies the design of a controller. Motor voltage is then described by an auxiliary equation.

All dynamic systems can be represented by a set of states or state variables which describe the system energies.[6] The energies can be divided into two basic classes: static/potential and dynamic/kinetic, or analogous terms. For example, the motor state can be described by armature position and rotational velocity. State equations are typically written in matrix notation. In particular, most forms of dynamic systems can be represented by two matrix equations:

$$\dot{\mathbf{x}}(t) = \mathbf{A}(\mathbf{x}, t)\,\mathbf{x}(t) + \mathbf{B}(\mathbf{x}, t)\,\mathbf{u}(t) \tag{1}$$

$$\mathbf{y}(t) = \mathbf{C}(\mathbf{x}, t)\,\mathbf{x}(t) + \mathbf{D}(\mathbf{x}, t)\,\mathbf{u}(t) \tag{2}$$

where $\mathbf{x}$ is the state variable vector and (1) is the "state equation." Matrix $\mathbf{A}(\mathbf{x}, t)$ describes the feedback part of the system and matrix $\mathbf{B}(\mathbf{x}, t)$ describes the feed forward part from the input vector $\mathbf{u}(t)$. The "output equation," (2), describes all auxiliary variables that may depend on the system state or input vector but do not affect the system state.

As an example, let us model the motor described earlier in state variable form, with a voltage source as the input. The mechanical state variables are motor shaft position and velocity, and electrical energy is best described by the current flowing in the inductance of the armature. Given these three state variables, the coefficients of the motor equation are

$$\mathbf{A} = \begin{bmatrix} 0 & 1 & 0 \\ 0 & -P/M & K_t/M \\ 0 & -K_e/L & -R/L \end{bmatrix} \tag{3}$$

$$\mathbf{B} = \begin{bmatrix} 0 \\ 0 \\ 1/L \end{bmatrix}, \tag{4}$$

where $K_t$ is the motor torque constant, $M$ is the armature moment of inertia, $P$ is the viscous friction coefficient, $K_e$ is the inducted back EMF coefficient (EMF = $K_e \times$ Vel), $L$ is armature inductance, the state variable vector is

$$\mathbf{x} = \begin{bmatrix} \text{armature position } (\theta) \\ \text{armature velocity } (\dot{\theta}) \\ \text{armature current I} \end{bmatrix}, \tag{5}$$

and the input $u(t) = V_s(t)$. The motor torque $T$ is a direct function of the armature current, giving for the output equation

$$T = y = \mathbf{C}\mathbf{x}(t) + \mathbf{D}u(t) = [0\ 0\ K_t]\mathbf{x}(t), \tag{6}$$

where $\mathbf{D} = 0$ in this case.

The third equation in (3) can be eliminated by driving the motor with a current source. The coefficients of the state equation become

$$\mathbf{A} = \begin{bmatrix} 0 & 1 \\ 0 & -P/M \end{bmatrix} \tag{7}$$

$$\mathbf{B} = \begin{bmatrix} 0 \\ K_t/M \end{bmatrix}, \tag{8}$$

where the state variable vector consists of armature position and velocity only, and the input $u(t) = I_s(t)$. The output equation becomes

$$T = \mathbf{D}u(t) = K_t I_s(t), \tag{9}$$

where $\mathbf{C} = 0$ in this case.

The control system is described in the next section. Details of the computer simulation are discussed in Section III. In Section IV the results of various parameter studies are presented. Section V describes some experiments with the completed gripper system. Finally, some concluding remarks concerning certain significant results are offered along with some plans for future study.

## II. GRIPPER CONTROL SYSTEM

The principal function of the controller is to position each gripper finger appropriately for approaching an object and to close the gripper fingers on the object. Another goal of the gripper control system design is to provide a means for affecting the mechanical properties so that gripper compliance and dynamic performance can be modified under computer control. For example, it is desirable to minimize impact forces due to the inertia of the gripper finger and motor armature masses while allowing rapid response in the mechanism. One way to reduce impact forces is to reduce the mass of the fingers. Since the mechanical mass of the mechanism has already been minimized by design, it is desirable to further reduce the effective mass of the system by appropriate control variable feedback.

The effective mass of the gripper mechanism can be controlled electrically by feeding back an acceleration term in the control system. It is well known that effective damping in the system is controlled by velocity feedback. This was the basis for an early design of the gripper control system. Subsequently, after nonlinear computer analysis of several system configurations, a system design evolved which is depicted in Fig. 2.

The control system for the gripper consists of an analog section and a digital interface. Analog feedback methods were chosen after numerous computer simulations indicated that a microprocessor would not be fast enough to perform the complicated control calculations necessary at a sufficiently high sample rate. The control circuitry consists of 24 operational amplifiers, six 8-bit Multiplying Digital-to-Analogue Converters (MDACs), two 10-bit DACs, and a digital interface. The digital interface communicates with a SUN 68000 microcomputer running under New Real-Time Executive (NRTX) operating system.[7] Mechanical compliance is controlled by position feedback, damping by velocity feedback, and effective mass by acceleration feedback. The velocity and acceleration signals are obtained from the position signal by electrical differentiation. In order for this technique to work well, the position signal must have very low noise. The

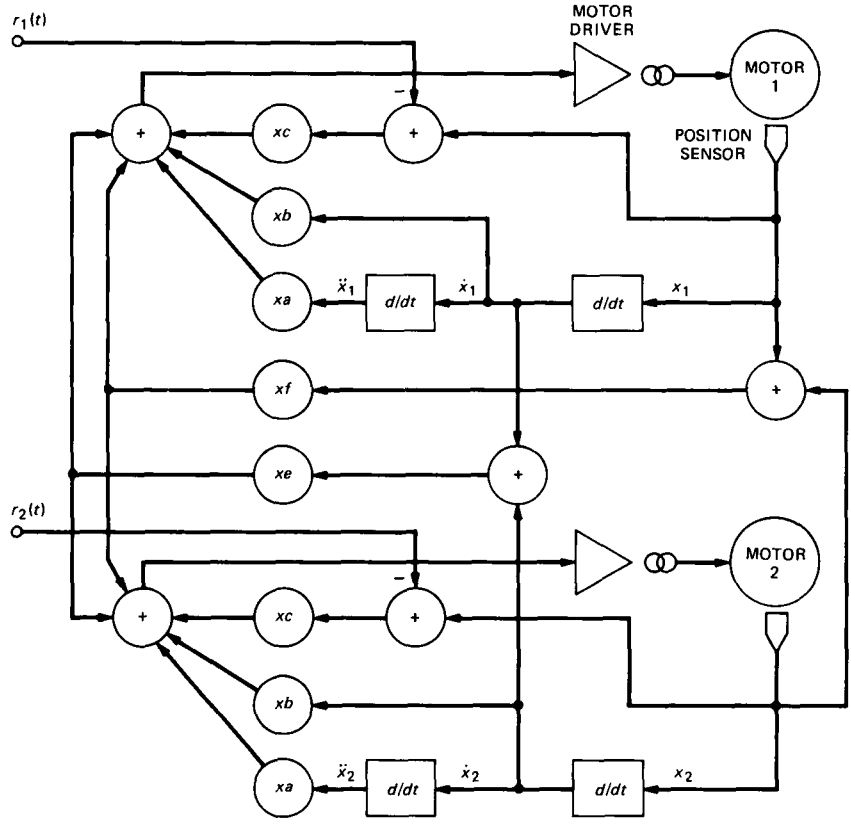


Fig. 2—Gripper control system.

amounts of position and velocity feedback are controlled by computer through the digital interface and 8-bit MDACs indicated by coefficients $b$ and $c$ in Fig. 2. Finger positioning stiffness is controllable from zero to about 23,000 N/m in increments of about 90 N/m. Acceleration feedback gain is fixed by a trimmer potentiometer and is set as high as possible consistent with stable operation of the gripper. Command positions [$r_1(t)$ and $r_2(t)$] are controlled by 10-bit DACs for a positioning resolution of about 40 $\mu$m.

An additional feature of the control system is a means of cross-coupling the two finger positions so that an effect on common-mode compliance is obtained. Common-mode damping is provided by common-mode velocity feedback. Both common-mode position and velocity gains are controlled by 8-bit MDACs (coefficients $e$ and $f$ in Fig. 2). This common-mode feedback allows the gripper fingers to, for example, hold an object with a soft grip (differential mode) while stiffly holding the object's position with respect to the gripper body

(common mode). Alternatively, the common-mode stiffness can be made zero so that the finger positions can conform to an off-center object when they are closing (such as a peg in a hole).

Common-mode compliance control can be illustrated by a few examples. Ignoring velocity and acceleration gains, the feedback equations for the gripper fingers are

$$I_1 = a_1(r_1 - x_1) + f(x_1 + x_2) \tag{10}$$

$$I_2 = a_2(r_2 - x_2) + f(x_1 + x_2), \tag{11}$$

where $I_1$ is the motor current control signal for motor 1 (which may be scaled by fixed gain constants), $a_1$ is position gain associated with finger 1, $f$ is the common-mode position gain, $r_1$ is the commanded position for finger 1, $x_1$ is the actual position of finger 1 (positive direction is motion toward the center of the gripper), and $x_2$ is the actual position of finger 2, etc. The gripper fingers always tend to move so that $I_1$ and $I_2$ are zero. The amount of deviation of the values of $I_1$ and $I_2$ from zero is proportional to the reactive force generated by the servomotor.

By appropriate choice of $a_1$, $a_2$, and $f$, several different modes of operation can be obtained. Under normal operating circumstances, the values for finger 1 ($a$, $b$, and $c$) are chosen to be the same as those of finger 2 for balanced operation. If $f$ is set to one half the value of $a$, for example, then the common-mode stiffness is very high and differential-mode stiffness is zero. The control equations become

$$I_1 = ar_1 + a(x_2 - x_1)/2 \tag{12}$$

$$I_2 = ar_2 + a(x_1 - x_2)/2, \tag{13}$$

where $a = a_1 = a_2$. This results in an effect where each finger individually has no stiffness with respect to the gripper body as long as the other finger is free to move. However, if both fingers are forced to move in the same direction, considerable stiffness is encountered. In this mode the fingers tend to stay equally distant from a position value centered between the two-finger command values $r_1$ and $r_2$. If the values of the $a$ coefficients are increased, a soft grip can be established with very firm centering of the object. This is useful when the robot arm is in motion as it keeps the fingers and object centered without unnecessary gripping force.

Alternatively, if the $a$ coefficients are made zero and $f$ is negative, common-mode stiffness is nullified and all stiffness appears as differential-mode stiffness. The control equations reduce to

$$I_1 = -a(x_1 + x_2) \tag{14}$$

$$I_2 = -a(x_1 + x_2). \tag{15}$$

This means that the gripper fingers are stiff with respect to each other, but exhibit no stiffness with respect to the gripper body. This mode of operation is particularly useful in picking up objects that may not be positioned exactly in the center of the gripper. The fingers will easily conform to the position of the object without applying significant lateral forces. Varying amounts of common-mode versus differential-mode stiffness can be obtained with values of $f$ between zero and one-half $a$.

We will introduce the state feedback control equations by first considering a single finger with position, velocity, and acceleration feedback with a current-driven servomotor. Initially, we will assume that the velocity and acceleration are available directly from the finger by appropriate sensors (later we will remove this requirement). We will also assume a linear system until later when nonlinearities are added. Then we can write a feedback equation for the motor current as follows:

$$I_s(t) = -a\ddot{y}(t) - b\dot{y}(t) - c[y(t) - r(t)], \tag{16}$$

where $r(t)$ is the reference position input function and $a$, $b$, and $c$ are gain coefficients. Substituting (16) into (7) through (8) and combining like terms yields

$$\mathbf{A} = \begin{bmatrix} 0 & 0 \\ -cK_t/(M + aK_t) & -(P + bK_t)/(M + aK_t) \end{bmatrix} \tag{17}$$

$$\mathbf{B} = \begin{bmatrix} 0 \\ cK_t/(M + aK_t) \end{bmatrix}, \tag{18}$$

where, again the state vector, $\mathbf{x}$, consists of finger position $\dot{y}$ and velocity $\dot{\dot{y}}$, and the input function $u(t) = r(t)$.

The lower left element of $\mathbf{A}$ is now nonzero, indicating that a position-sensitive term is present. This term is effectively a spring constant divided by a mass. For comparison, examine the state equations for a classical elementary mass, spring, and damper problem:

$$\mathbf{A} = \begin{bmatrix} 0 & 1 \\ -k/m & -p/m \end{bmatrix} \tag{19}$$

$$\mathbf{B} = \begin{bmatrix} 0 \\ 1/m \end{bmatrix}, \tag{20}$$

where $k$ is the spring constant, $p$ is the damping coefficient, and $m$ is the mass. The input function $u(t)$ applies a force to the mass, which is attached to a stationary support by the spring and damper. Note that in (17) through (18) the spring constant is replaced by $(cK_t)$, the damping by $(P + bK_t)$, and the mass by $(M + aK_t)$. Thus, these

mechanical parameters can be independently controlled by the electrical feedback gains ($a$, $b$, and $c$) in the control system.

The second finger is controlled in a similar manner. The two fingers thus operate independently in this case. Figure 2 also shows control signal passing from each finger to the other. These signal paths provide additional common-mode position and velocity feedback, which increases the common-mode stiffness. It was found, during computer simulation, that common-mode acceleration was not useful and that it tended to destabilize the control system. The complete feedback equation for motor drive current is

$$I_s(t) = -(a + d)\dot{y}_1(t) - d\dot{y}_2(t) - (b + e)\dot{y}_1(t) - e\dot{y}_2(t) \\ -(c + f)y_1(t) - fy_2(t) + (c + f)u_1(t) + fu_2(t). \quad (21)$$

Closed-form solutions of the above equations are not readily obtainable for a nonlinear system. The construction of our gripper involves servomotors with power limitations. The motor driver has both voltage and current limitations (which must be treated separately). The rack and pinion have backlash, and the mechanical parameters change abruptly when an object is grasped. The rack and pinion gear backlash has turned out to be a small effect, but it was not initially clear if this hysteretic effect would cause system instability with the electrical feedback.

## III. COMPUTER SIMULATION

A fourth-order Runge-Kutta algorithm was used to study the time response of the nonlinear system just described. The algorithm used is modified somewhat from standard routines found in the literature and is described in Appendix A. The state equations must be expanded to include the various nonlinearities. After doing so, the two-fingered model requires an eight-dimensional state vector. Figure 3 is a diagram of the model and includes an object to grasp (in this case a rubber ball). For the time being, we will still assume that the finger velocity and acceleration are directly available. Later, we will study the influence of electrical time constants on the mechanical performance.

The model shown in Fig. 3 consists of five mechanically independent members. They are the two fingers, two motor armatures, and the rubber ball. Each mechanical member will require two state variables to describe its position and velocity. The ten-dimensional state vector is

1. Left finger position
2. Left finger velocity
3. Left armature position

4. Left armature velocity
5. Right finger position
6. Right finger velocity
7. Right armature position
8. Right armature velocity
9. Ball position
10. Ball velocity.

The state equation describes forces that exist on each mechanical member. These forces may be due to acceleration, frictional drag, or spring forces. Also included are forces applied to each member by another member when they are in contact. To introduce the state feedback matrix, let us first consider the case where no contact is being made between any of the mechanical members and the common-mode feedback is ignored. Then the coefficients of the state equation are

$$\mathbf{A} = \begin{vmatrix} 0 & 1 & 0 & 0 & 0 & 0 & 0 & 0 & 0 & 0 \\ 0^* & -P/M^* & 0^* & 0^* & 0 & 0 & 0 & 0 & 0^* & 0^* \\ 0 & 0 & 0 & 1 & 0 & 0 & 0 & 0 & 0 & 0 \\ -c\,K_t/m^* & -b\,K_t/m^* & 0^* & -p/m^* & 0 & 0 & 0 & 0 & 0 & 0 \\ 0 & 0 & 0 & 0 & 0 & 1 & 0 & 0 & 0 & 0 \\ 0 & 0 & 0 & 0 & 0^* & -P/M^* & 0^* & 0^* & 0^* & 0^* \\ 0 & 0 & 0 & 0 & 0 & 0 & 0 & 1 & 0 & 0 \\ 0 & 0 & 0 & 0 & -c\,K_t/m^* & -b\,K_t/m^* & 0^* & -p/m^* & 0 & 0 \\ 0 & 0 & 0 & 0 & 0 & 0 & 0 & 0 & 0 & 1 \\ 0^* & 0^* & 0 & 0 & 0^* & 0^* & 0 & 0 & 0^* & 0^* \end{vmatrix} \tag{22}$$

$$\mathbf{B} = \begin{bmatrix} 0 & 0 & 0 & 0 \\ 0 & 0 & 0 & 0 \\ 0 & 0 & 0 & 0 \\ K_t & 0 & -a\,K_t/m & 0 \\ 0 & 0 & 0 & 0 \\ 0 & 0 & 0 & 0 \\ 0 & 0 & 0 & 0 \\ 0 & K_t & 0 & -a\,K_t/m \\ 0 & 0 & 0 & 0 \\ 0 & 0 & 0 & 0 \end{bmatrix}, \tag{23}$$

where $P$ is the damping coefficient of the finger slide mechanism, $M$ is the mass of the finger, $p$ is the damping coefficient of the motor armature, and $m$ is the mass of the armature. The rubber ball rolls on a table with negligible friction.

The input function $\mathbf{u}(t)$ is a vector of four dimensions. The first two dimensions are the left and right finger position reference inputs. The last two dimensions are inputs from the implied left and right accelerometer sensors. This variation of the feedback equation is useful since acceleration is not one of the state variables available. Alternatively, the time derivative operator could be used in the $\mathbf{A}(\mathbf{x}, t)$ matrix.

The $\mathbf{A}(\mathbf{x}, t)$ matrix becomes more complicated when any of the

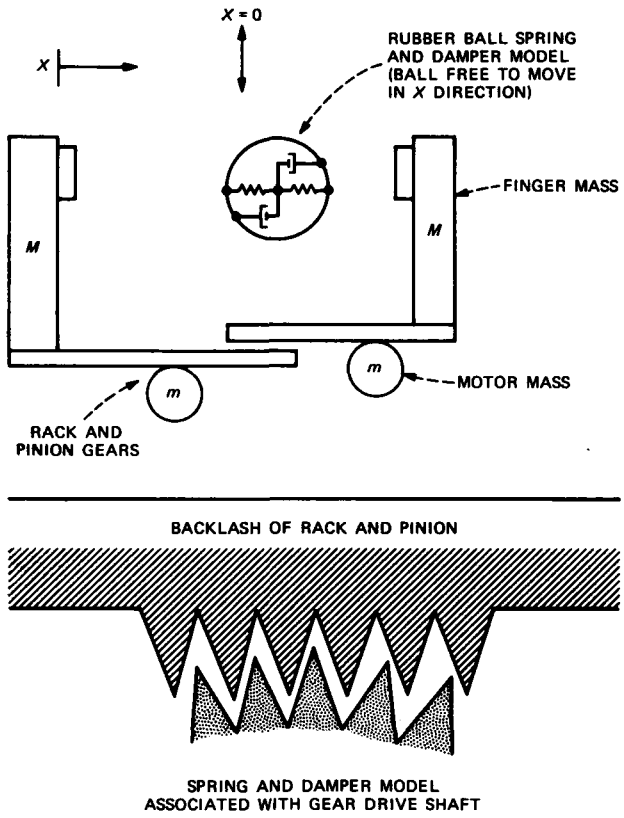


**Fig. 3—Model of two-fingered gripper.**

mechanical elements come into contact. Some or all of the elements of the matrix indicated with an asterisk in (22) become nonzero, and additional forces are coupled to the various mechanical parts in a symmetric manner. Equal and opposite forces are introduced into two rows of $\mathbf{A}(\mathbf{x}, t)$ when contacts are made. Thus, the matrix form of (22) is helpful in illustrating the symmetry in the problem. For example, when the left finger contacts the ball, elements 1, 2, 9, and 10 of row 4 are affected. At the same time, the corresponding elements of row 10 are also affected with identical magnitude, but with opposite signs. The motor drive nonlinearities are saturation limits on both voltage and current. These enter directly into the motor torque equations.

The actual nonlinear state equation would consume more than a single page. A C program listing of the complete state equation is given in Appendix B. This listing of the state equation also includes the electrical time constants, which deserve some discussion.

Heretofore, we had implied that the acceleration of the left and right fingers would be available via some sensor, such as an accelerometer. In the actual gripper design, the acceleration and velocity are obtained by electrical differentiation of signal from the position sensor. The design of an electrical differentiator purposely incorporates a pole in the transfer function to limit the high frequency gain and thus reduce the amount of noise developed by or passed through the circuit. It is desirable to make this frequency limit as low as possible to minimize the circuit noise. However, the accuracy of the differentiation may suffer if the pole location is too low in frequency. An analysis of the effects of differentiator pole position was therefore necessary. The motor drive amplifier also has a dominant pole at a moderately low frequency (about 1500 Hz) and its effect is also included in the state equation.

## IV. RESULTS OF THE SIMULATION

Transient response analysis was performed for various parameter settings to determine the effects of different amounts of feedback, the effects of various ball masses and compliances, and the effects of the differentiator time constants. A fourth-order Runge-Kutta algorithm was employed with modifications of the step size correction algorithm as described in Appendix A. The time response output is presented in graphical form that is easily read and gives a good indication of the performance.

Several parameters were initially established for the analysis. These include the mechanical specifications for the dc servomotors and the finger mechanisms. The servomotors were selected for this application based on their physical size, torque capability, and the fact that they are completely characterized by the manufacturer. The published specifications for the motors are

| | | | |
|---|---|---|---|
| Armature resistance | ($Ra$) | 6.12 | Ω |
| Armature inductance | ($La$) | 0.00275 | H |
| Motor EMF constant | ($Ka$) | 0.0446 | V-s/rad |
| Motor torque constant | ($Km$) | 0.0446 | N-m/A |
| Armature inertia | ($m$) | $1.54 \times 10^{-6}$ | N-m-s$^2$/rad |
| Armature damping | ($p$) | $2.74 \times 10^{-6}$ | N-m-s/rad. |

The symbols in parentheses refer to variables in the computer program (Appendix B). In addition, specifications for the rack and pinion gear mechanism used are

| | | | |
|---|---|---|---|
| Pinion gear radius | ($rg$) | 0.0081 | m |
| Pinion gear backlash | ($H$) | $5.08 \times 10^{-5}$ | m |
| Finger mass | ($M$) | 0.6 | kg |
| Finger damping | ($P$) | 0.5 | N-s/m. |

The following parameters are variable in the simulation and can be set to establish interesting initial conditions:

(a) Mechanical parameters:

| | |
|---|---|
| Initial ball position | ($y$[8]) |
| Ball radius | ($R$) |
| Ball stiffness | ($k3$) |
| Ball mass | ($m3$) |
| Ball damping | ($p3$) |

(b) Electrical parameters:

| | |
|---|---|
| RC time constants | ($RC$) |
| Position feedback gain for each finger | ($c$) |
| Velocity feedback gain | ($b$) |
| Acceleration feedback gain | ($a$) |
| Common-mode position gain | ($f$) |
| Common-mode velocity gain | ($e$) |
| Common-mode acceleration gain | ($d$) |
| Motor driver voltage limit | ($V$max) |
| Motor driver current limit | ($I$max). |

Several of these items introduce nonlinearities into the state equation. Two voltage programmable power supplies were used for motor drivers. These power supplies are linear units capable of operating either as voltage or current sources. The supplies used in this study are limited to 50 volts and/or 8 amperes. They can operate as either a power source or sink. They can also be controlled by either a voltage input or via a digital port, making them useful for microprocessor control.

Initially, the transient analysis is conducted with step position command inputs. Later, we will discuss exponential input functions and their effect on performance. To perform a typical simulation the initial conditions are set so that the gripper is in the fully open position. Thus, the gripper is opened to a width of 6.35 cm. The step input functions are then applied and the gripper closes on an object, in this case the ball. Time responses of each finger and the ball position are computed along with the associated motor voltages and currents. Also calculated are the ball position (and velocity), the impact force being applied to the ball by each finger, and the estimation errors of the electrical differentiators. This information is all displayed on a single page in graphical form for each test response.

The gripper was designed to allow each finger to move 3.8 cm. The fingers have about 1.25 cm of travel overlap, so in the fully opened position they are about 6.35 cm apart. The positional reference for the

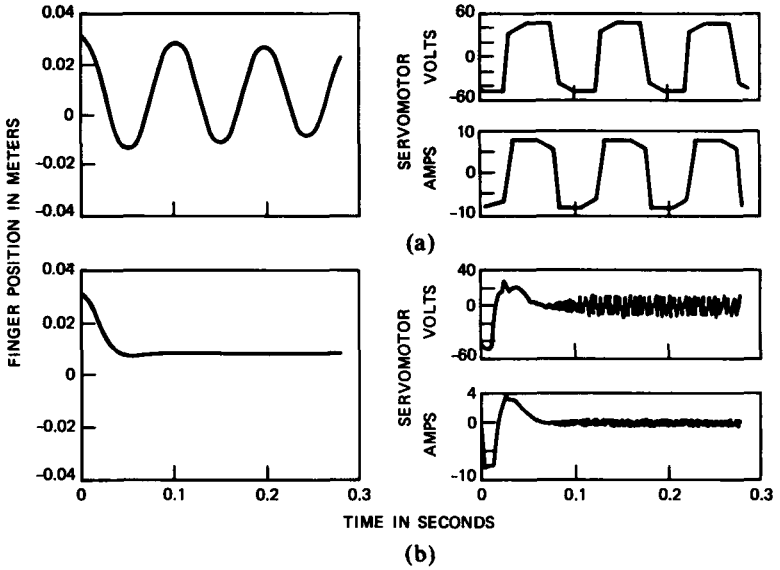


Fig. 4—(a) Step response with position feedback. (b) Step response with position and velocity feedback.

fingers was established so that the closed position of the gripper with the fingers centered is considered the zero position of each finger. The left finger opens in the minus $x$ direction and the right finger opens in the plus $x$ direction.

Figure 4 illustrates the effects of power supply limits, gear backlash, and velocity feedback on the time response. For these responses the gear backlash was set to 1 mm to make the hysteresis effect obvious. This is roughly equivalent to removing every other tooth from the gear. Figure 4a shows a response with position feedback only. Without velocity feedback the mechanical damping is obviously inadequate. The gear backlash is only slightly visible in the plot of position versus time and appears as a slight jaggedness in the response. The voltage and current plots show the effects of the motor driver limits and the inductance of the motor. Note that initially the voltage is saturated at −50 volts. The current goes to nearly −8 amps but then decreases until the driver switches to +8 amps. This ramp effect is due to the induced back EMF of the motor as it gains velocity. The voltage response shows similar characteristics during current saturation.

Figure 4b shows a response with viscous damping applied by velocity feedback. In this case the velocity gain is set to properly complement the position gain so that settling time of the finger is somewhat less than "critically damped." This amount of damping results in minimum settling time to the final position since a very slight amount of

overshoot in the response (a few percent) results in much faster convergence to the desired control point. The effects of gear backlash can now be seen in the voltage and current plots. During the dynamic part of the response there is very little evidence of gear backlash. The gear is first in contact on the forward thrusting (accelerating) face and then on the decelerating face. After the position of the finger becomes stable, the gear must continually switch faces to maintain the finger in position. This backlash effect shows up as a small oscillation in the drive current and voltage. The actual gear backlash of the gripper is much smaller than this and its effect will not be apparent in the time responses that follow.

When the fingers come into contact with the ball, impact energy and forces are exerted that may cause damage to the ball (or object) and/or gripper mechanism. These impact forces can be affected significantly by acceleration feedback. Figure 5 illustrates this effect. A typical damped closure of the gripper is shown in Fig. 5a. The gripper is set in the fully open position and closes on a 2-cm diameter ball weighing 0.5 kg. The impact forces are quite high, several times the magnitude of the final static gripping force applied by the servomotors. Figure 5b shows what happens when the mass is reduced by positive acceleration feedback. The amount of positive feedback must be carefully controlled or effective mass will become negative and result in oscillations. For the results of Fig. 5 the acceleration gain has been adjusted to reduce the effective mass to about 10 percent of the true mass. The impact forces have been reduced by acceleration feedback, but the amount of reduction is dependent upon properties of the rubber ball and other feedback parameters. Under good conditions, impact forces can be reduced by almost 50 percent.

There are two significant differences in the responses of Figs. 5a and b. First, the initial peak impact force has been reduced from 50N to about 20N with acceleration feedback. Furthermore, the gripper stabilizes the ball position much more rapidly. This is due to the increased responsiveness of the gripper fingers to the ball dynamics as a result of the reduced effective mass. Increased motor drive bandwidth is also required in order to control the effective mass. Note the high frequency components present in the drive currents of Fig. 5b.

A series of test simulations were conducted for various rubber ball stiffnesses and damping coefficients to investigate the effectiveness of acceleration feedback. Again, simulations were performed using a step function position control input. The ball is positioned 1 cm off-center toward the right finger in order to test the ability of the gripper to center and stabilize the position of the ball. The position feedback gain was set to 500 amps per meter (which is equivalent to a spring

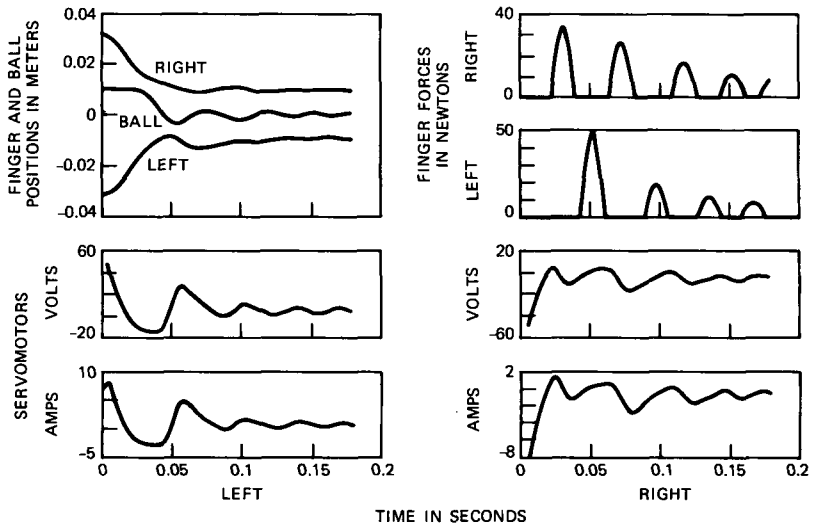


(a)

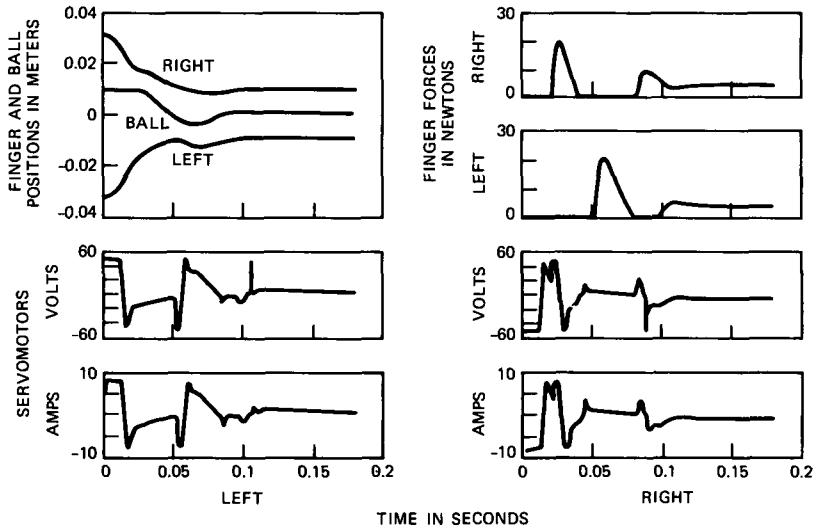


(b)

Fig. 5—(a) Damped gripper closure with position and velocity feedback. (b) Damped gripper closure with position, velocity, and acceleration feedback.

rate of about 2750 N/m) for the first two test series, and critical damping was established by a velocity feedback of 14.95 A-s/m.

The ball damping was set to 1.0 N-s/m for the first test series. The ball stiffness was varied from $10^2$ N/m to $10^6$ N/m. Acceleration feedback was set to reduce effective mass to about 5 percent of

mechanical mass at 0.11 A-s$^2$/m. The ratio of peak impact force applied by the first contact between a gripper finger and the ball with and without acceleration feedback was taken to be the measure of the effectiveness of this feedback. The results of this test series are plotted in Fig. 6a. The plot shows that the ball stiffness has a substantial influence on the effectiveness of acceleration feedback. Peak impact force is only slightly reduced for very large or very small stiffnesses. The effect is substantial at moderate stiffness ($10^4$ N/m) but only over a narrow range.

A second series of tests were conducted with the stiffness fixed at $10^4$ N/m. The ratio of impact forces was plotted again for ball damping from 0.01 to $10^4$ N-s/m. Figure 6b shows that damping has little effect on the impact ratio until it exceeds about 10 N-s/m. After this point is reached, electrical damping predominates over the stiffness. At very large damping values the acceleration feedback becomes totally ineffective.

The position feedback was varied in a third set of test simulations. The ball stiffness was fixed at $10^4$ N/m and the damping was set at 1 N-s/m. Velocity feedback was adjusted in each instance so that critical damping was maintained. Figure 7 shows a plot of the results for position feedback gains varying from 10 to 5000. Both very low and very high gains appear to adversely influence the effectiveness of acceleration feedback. Position feedback gains in the range of 50 to 200 A/m have the greatest effect.

Since position feedback produces an effect similar to the stiffness of the ball, it is not surprising that the plots have similar characteristics. Loss of acceleration feedback effectiveness at high stiffnesses can be attributed to relatively slow response time of the servomotors in comparison to the mechanical resonance of the ball and finger system. Since it takes approximately 100 $\mu$s for the servomotors to reverse the gear force (because of backlash), the mechanism simply does not have enough time to counteract the effects of the real mass of the fingers. Poor acceleration feedback effectiveness at very low stiffnesses appears to be due to mismatch between the stiffnesses of the finger and the ball. If one of the stiffnesses overwhelms the other, particularly by several orders of magnitude, the acceleration feedback becomes useless.

Another means for reducing impact forces is to bring the fingers into contact with the ball at low velocity. This could be accomplished by simply bringing the fingers slowly together by applying a ramp function to the position control inputs; however, this makes the gripper operation slow. Since it is only necessary for velocity to be low just before contact is made with the ball, another possibility is to increase the negative velocity feedback so that the finger system is overdamped.

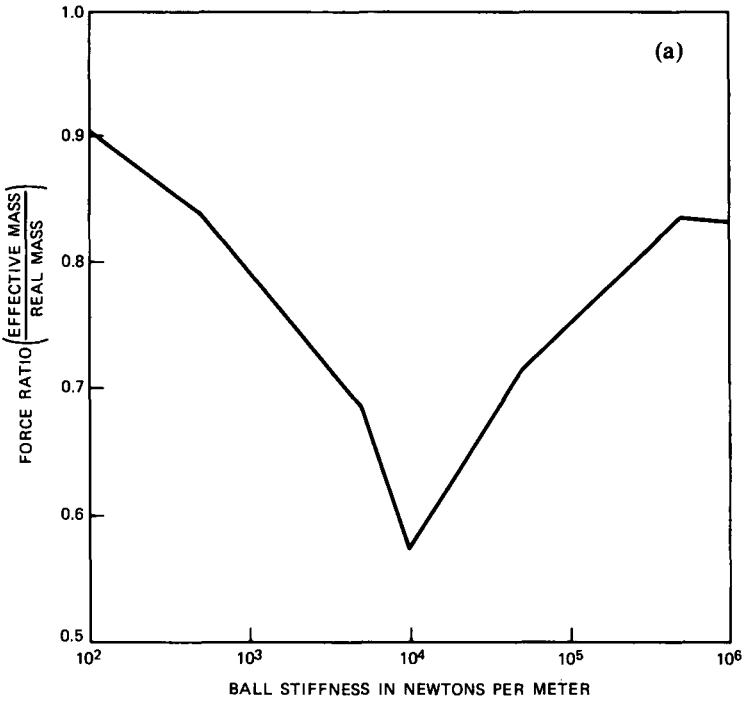


Fig. 6—(a) Peak impact force ratio versus ball stiffness. (Cont.)

This results in an exponential velocity response. However, computer simulation shows that this does not really reduce impact forces, since the fingers become very resistive to springy impacts. The series of Fig. 6b illustrates this. Another alternative is to apply an exponential position control input to each finger. This takes advantage of the higher allowed velocity and slows the fingers down as they approach the contact points. Furthermore, these input functions are very easy to generate in hardware. Figure 8 shows an example of combined positive acceleration feedback and exponential control input functions with 50-ms time constants. The impact forces are now reduced to little more than the final static gripping force. Several time constants for the input exponentials were investigated, and the 50-ms exponential appeared to yield the best overall results (low impact force consistent with rapid closure) for this particular mechanical gripper.

An analysis of sampling period was performed on a discrete time control architecture to determine if the gripper could be controlled adequately by a microprocessor. This was accomplished by modeling the motor drivers as zero-order sample and hold devices. A minimum sample rate of at least 5000 samples per second was indicated by numerous computed responses. This rate would be needed to control

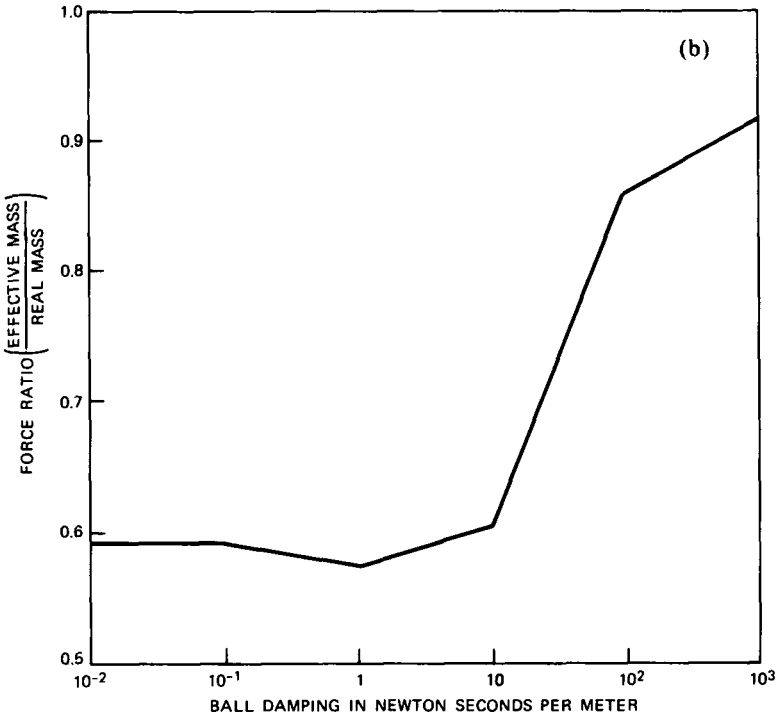

Fig. 6—(b) Peak impact force ratio versus ball damping.

the gripper without loss in performance. This requirement could be relaxed somewhat if certain erroneous dynamic response characteristics could be tolerated; however, the characteristics observed in the simulation were not considered acceptable. This sample rate would only be possible for a microprocessor if a very simple control strategy were being implemented. Computing the motor currents necessary every 200 $\mu$s for the more sophisticated feedback strategy being planned is more than a normal microprocessor can handle. (It is possible to perform the operations with a digital signal processor, however.) Consequently, the controller design is primarily analog, with digital-to-analog converters to allow a microprocessor to control the various feedback gains and apply position control inputs.

A conference on robot manipulators[8] triggered some thinking on the concept of differing common-mode and differential-mode compliance. Active compliance in our gripper is useful as long as the robot arm is not moving. When the robot arm does move, however, this previously useful compliance becomes a liability because the fingers of the gripper will swing from side to side under the acceleration influence of the arm motion. It is desirable to maintain the compliance relative to the grasped object and simultaneously keep the fingers and object from

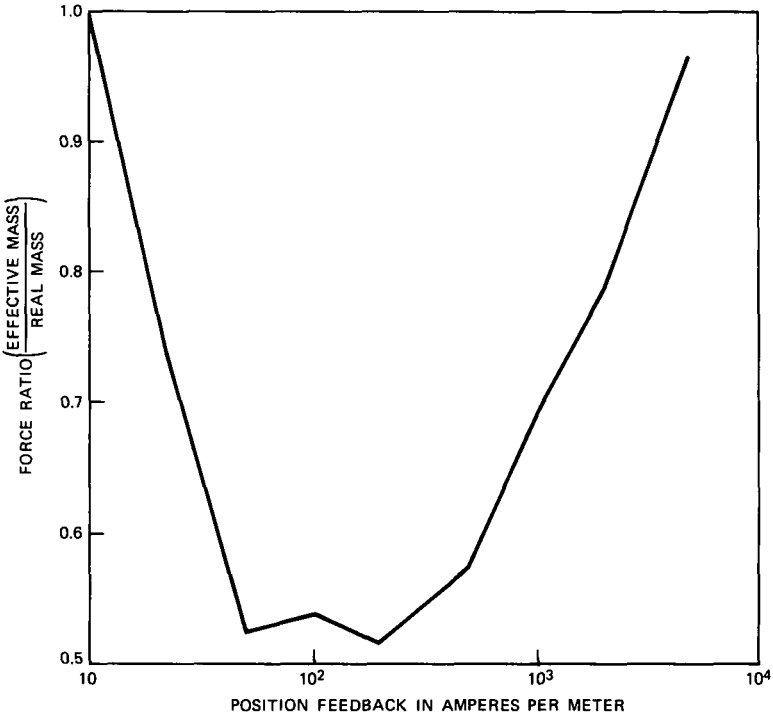


Fig. 7—Peak impact force ratio versus position feedback gain (critically damped).

swinging. This can be accomplished with appropriate common-mode feedback as discussed in Section II.

The effect of additional common-mode stiffness is illustrated in Fig. 9. This should be compared to Fig. 5a. Both common-mode position and common-mode velocity feedback are necessary for suitable common-mode performance. The initial conditions have been set to the same values as in previous tests. Inertia of the ball causes the gripper to accommodate somewhat to the position of the object and close slightly off-center. The object is then forced to the center by the common-mode stiffness. Close inspection of the position plot of Fig. 5a shows some common-mode finger oscillation under the influence of the ball vibration. This common-mode component is almost entirely eliminated in Fig. 9. Further experiments simulating arm motion by applying common-mode variations to the position control input functions indicate that the increased common-mode stiffness significantly reduces the amount of arm motion influence on the fingers.

We had previously assumed that velocity and acceleration signals were available from appropriate sensors such as tachometers and accelerometers. The actual gripper uses a position sensor that consists

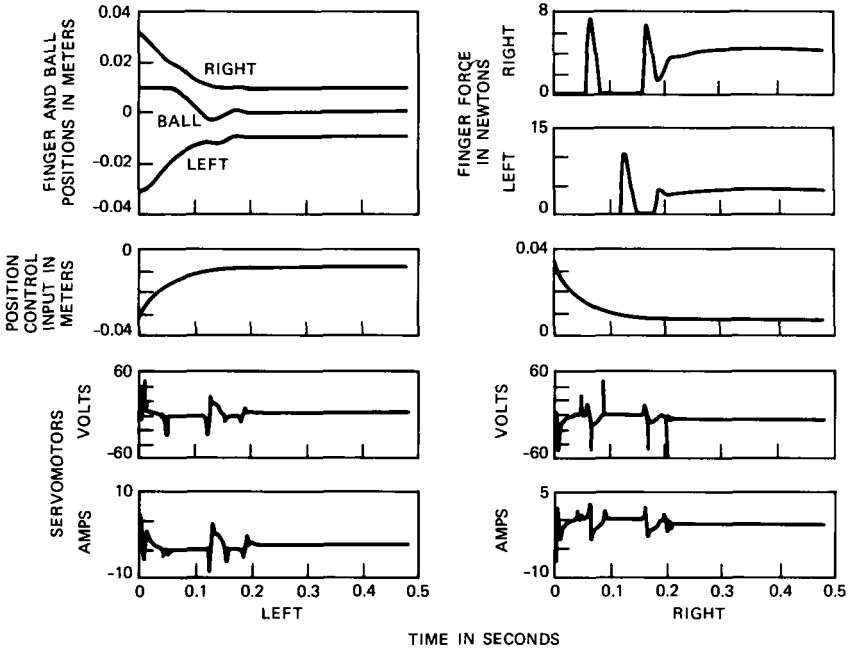


Fig. 8—Damped closure with 50 milliseconds time constant.

of a capacitive measurement device described by G. L. Miller.[5] The velocity and acceleration signals are obtained electronically from the position signal by electrical differentiation. It is desirable to limit the high-frequency gain of the differentiator circuits used to estimate these parameters, so electrical poles are purposely designed into the differentiator transfer functions. Extensive computer simulation has shown that the electrical time constants should not exceed 100 $\mu$s. Figure 10 shows a time response for circuit time constants of 10 ms. This should be compared to Fig. 9. The obvious distortion of the mechanical response is further indicated in the log error plots of velocity and acceleration estimates for the right finger. The errors are typically no more than about 10 percent for circuit time constants of 100 $\mu$s, and the mechanical response is virtually identical to responses obtained with smaller time constants.

## V. TESTING THE GRIPPER

Initial tests conducted on the gripper showed that high-frequency noise was present in the position signal. Although the level of this noise was low (about 50 dB s/n), it became important when used to determine the velocity and acceleration signals. At the acceleration output of the differentiators, the wideband noise level was only 30 dB

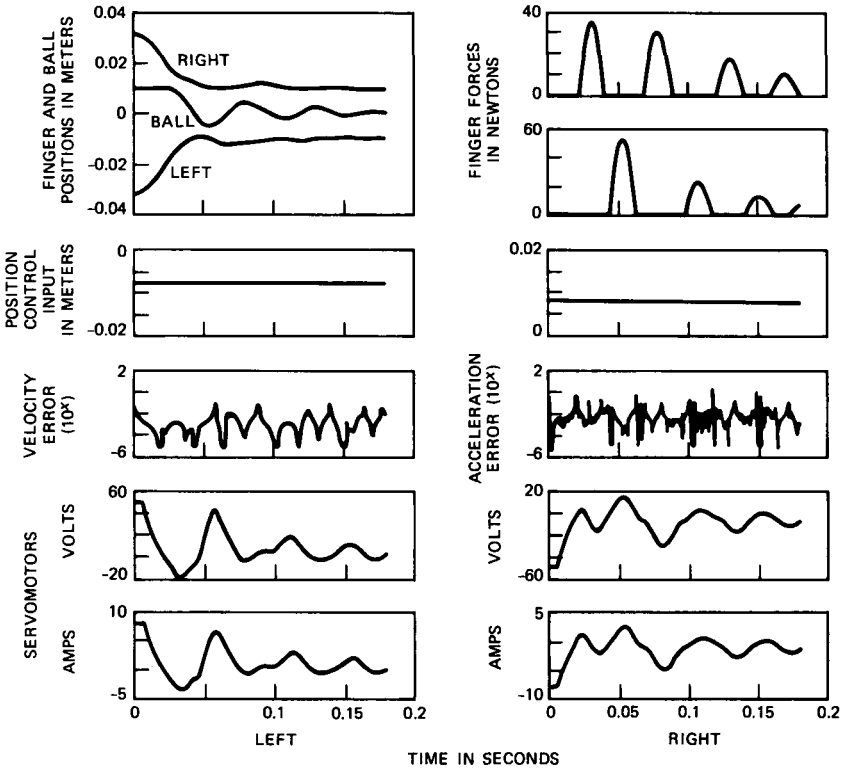


Fig. 9—Damped gripper closure with common-mode feedback.

below the signal, a level high enough to cause gear chatter in the rack and pinion drive. Subsequent modifications of the position sensing circuitry reduced this noise level to about 90 dB below signal, which made the acceleration signal useful for feedback purposes.

To verify the simulation results, measurements of the mechanical finger mass and damping were necessary. This was accomplished by performing underdamped step response tests on the gripper. Figure 11 shows a typical underdamped step response. This response is very much like that of a simple mass, spring, and damper. The mass can be determined from the resonant frequency and the damping from the rate of decay in the response. Undamped resonant frequency is given by

$$\omega^2 = \frac{k}{m}, \tag{24}$$

where $\omega$ is frequency in radians per second, $k$ is the spring constant in Newtons per meter, and $m$ is mass in kilograms. Damping (N-s/m) can be determined from

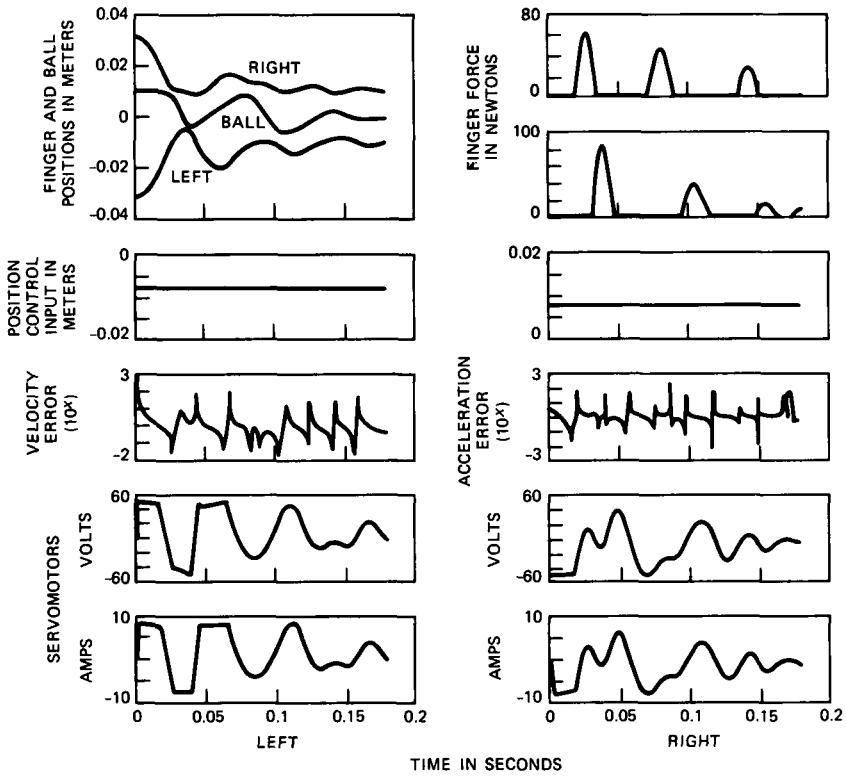


Fig. 10—Damped gripper with common-mode feedback and 10 milliseconds electrical time constants.

$$b = \frac{2m}{T} \ln \frac{x_1}{x_2}, \tag{25}$$

where $b$ is the damping in Newton-seconds per meter, $m$ is the mass in kilograms, $x_1$ and $x_2$ are successive peak amplitudes in the decaying response, and $T$ is the cycle period in seconds.

There remains the problem of verifying the spring constant, which, in this case, is due to the position feedback through the servomotor. Although the motor is completely characterized by the manufacturer, it was deemed important to measure the spring constant actually obtained from the servomotor. This was accomplished by performing a step response analysis with two different masses attached to the motor through the rack and pinion, as follows:

Let $m_1$ = finger mass

$m_2$ = slide and motor mass.

Then,

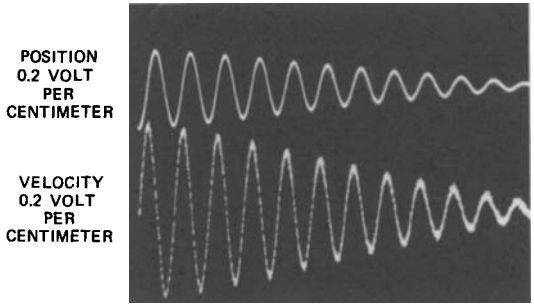


Fig. 11—Underdamped step response.

$$\omega_1^2 = \frac{k}{m_1 + m_2} \tag{26}$$

gives the undamped resonant frequency of the complete motor, slide bearing, and finger masses for a given equivalent spring constant $k$. The finger mass $m_1$ can be removed, leaving $m_2$ and a second resonant frequency $\omega_2$. Thus an equation for $k$ can be derived:

$$k = \frac{m_1}{\frac{1}{\omega_1^2} - \frac{1}{\omega_2^2}}. \tag{27}$$

Mass $m_1$ is measurable since it can be removed from the rest of the mechanism. Mass $m_2$ consists of a combination of the slide mechanism, the rack mass, and the gear and motor inertia. Once $k$ is determined, then $m_2$ can be calculated from (26).

Measurements in the laboratory yielded the following data:

$$\begin{aligned} k &= 3900 \text{ N/m} \\ m_1 &= 33.12 \text{ g} \\ \omega_1 &= 154.2 \text{ rad/s} \\ \omega_2 &= 172.6 \text{ rad/s} \\ m_2 &= 131 \text{ g}. \end{aligned}$$

A calculation of the gear inertia was made from the size of the gear and the density of steel (equivalent mass: 3.5 grams). Adding this to the published specification for the motor inertia and translating into the linear (rack) units yields a slide mass of 104 grams. Thus the total slide and finger mass is about 137 grams. The servomotor inertia with the gear attached is about $1.77 \times 10^{-6}$ kg $-$ m$^2$. With these parameters determined, the simulation program was used to verify the resonant frequencies.

Simulation results compared closely with the actual performance of the gripper. Typical step response settling times of 30 ms were obtained for high-position feedback gains, as predicted by the computer simulations. Absolute positioning accuracy is dependent upon the position sensor accuracy and mechanical imperfections. The currently employed sensor has a maximum error of about 0.5 mm.

Several slight differences in response between the actual gripper and the simulation were noted. The computer simulation did not consider the effect of static friction on the dynamic response. In this case, the frictional force appears to be a constant independent of velocity. With viscous friction, the underdamped response decays exponentially. Static friction results in a linear decay. The actual gripper responses indicate that a slight amount of static friction is present in the mechanism. The amount of static friction present is negligible for normally damped responses (near critical damping) since the viscous friction is dominant under these conditions. However, static friction does become significant when the finger compliance is high. This results in a positioning error, since the force necessary to overcome the static friction is proportional to the spring constant applied to the finger. One well-known method of solving this problem is to introduce high-frequency dither into the motor drive. The amplitude of the dither must be just sufficient to exceed the force necessary to break the static friction free. If the dither frequency is sufficiently high, its effect will not be seen in the finger position due to the inertia of the mechanism. Experiments with dither in the laboratory indicate that static friction is not the only source of positioning error.

Dither was found to be an effective means for obtaining higher positioning accuracy in the presence of static friction at low-position feedback gains (low spring constant); however, magnet detent action in the servomotor due to the magnetic reluctance of the armature poles also causes positioning error. The effect of this motor phenomenon is the appearance of virtual potential energy wells at uniform intervals along the finger track. Thus, the positioning error can be positive or negative, depending on the commanded position and the relative position of the nearest potential energy well. This effect can be compensated by adjusting the command position slightly, but it is nearly impossible to position the finger at a potential energy peak since any slight change in position can cause a change in sign of the detent force, which requires dynamic compensation. The only practical solutions for this problem are to increase the position feedback (which provides the dynamic compensation) of the system or reduce the motor gear radius so that the detents are closer together. The difficulty in electronically compensating for the detent action arises from the fact that there is no way of distinguishing between internally and externally

generated finger displacements with the present sensors. The current version of the gripper exhibits positioning detents at about 4 mm intervals.

The effect of acceleration feedback was tested by studying the underdamped step response of the gripper fingers with a known position feedback gain. The frequency of the response is an indication of the effective mass of the system. It was found that the resonant frequency could be increased by about 20 percent, indicating an effective mass change of

$$\frac{m_2}{m_1} = \frac{\omega_1^2}{\omega_2^2} = 0.64, \tag{28}$$

or about a 36 percent decrease in mass. The simulation predicted a somewhat higher mass reduction (about 55 percent), but it had not considered the effects of position measurement noise, which limited stable feedback gain.

Position measurement noise also becomes significant in the velocity feedback term when velocity gain is high (high damping). When position feedback gain is set to a high level, high-velocity gain is needed to obtain critical damping. Under these conditions the noise present in the position signal causes servomotor gear chatter. This gear chatter has no significant effect on the positioning accuracy or dynamic response of the gripper, but it does produce annoying sounds in the rack and pinion mechanism when the finger is not in contact with an object and is motionless. The high damping in the finger is not generally needed except when the finger is moving. Under computer control, it was found that the dynamic response of the finger is not affected if the high-velocity gain is present for only about 50 ms after the "move finger" command is initiated. Then the velocity gain can be reduced to a safe level for noise-free operation.

To make control of the gripper easier for the user a set of computer routines were written in the C language. These procedures allow the user to set all feedback parameters directly or, at a higher level, to move the fingers without having to be concerned with determining the appropriate velocity feedback for critically damped response. Velocity gain for critical damping can be determined from an equation of the form

$$b = k_1\sqrt{c} - k_2, \tag{29}$$

where $b$ is velocity gain, $c$ is position gain, and $k_1$ and $k_2$ are constants. Constant $k_2$ is due to the mechanical damping already present. Another slower procedure provides a method for opening and closing the fingers slowly by incrementally stepping the fingers to the command position. More sophisticated algorithms allow the user to specify a compliance

and gripping force to be applied when closing. The gripper is closed on the object and the applied force is increased to the specified amount.

## VI. SUMMARY

A robot gripper and mechanical impedance control system has been constructed based on the results of computer simulations. The computer simulation is an accurate and useful tool for studying the dynamic behavior of the gripper. It allows one to investigate various performance properties of the mechanical system (i.e., conduct computer experiments) without taking the risk of damaging components of the system or incurring the expense of building experimental equipment. The simulation could be improved somewhat by including the effects of static friction, the servomotor detent action, and the control system generated noise.

The controlled impedance gripper has an adjustable finger positioning stiffness that can be set in steps of about 90 N/m up to 23,000 N/m. Damping can be set accordingly by computer so that near critically damped response is obtained. The effective finger mass can be reduced by acceleration feedback to about 64 percent of its true value. This helps to reduce impact forces when the gripper fingers are closed on an object.

A computer algorithm library was devised to provide a user interface to the gripper control system. With this library a user can establish operating parameters for the gripper and move the fingers with critically damped responses without having to know the necessary velocity feedback parameters. Because of noise in the position measurement system, high-velocity feedback gains cause servomotor gear chatter. An algorithm has been developed to allow critically damped responses at high-velocity feedback gains by applying the velocity gain only during the transient period, after which the velocity feedback gain is reduced to a statically stable level. In this way the chatter was eliminated.

Improvements can be made to the gripper and control system to reduce the effects of static friction and motor detent action. Dither (high-frequency perturbation) of sufficient amplitude can reduce the effect of static friction. Smaller gear diameters will allow more accurate positioning of the fingers since detent positions will be more closely spaced in finger coordinates.

Adaptive control strategies are likely to be useful in future studies of the problems of robotic gripping. This becomes particularly important for manipulating objects of varying masses and physical dimensions. Knowledge of the size of objects being grasped may not, in general, be known in advance. This means that the gripper will have to adjust position feedback and/or control inputs to maintain a desired

gripping pressure on an unknown object. Further adaptations may improve the ability of the gripper to maintain the object in a stable position as the robot arm is moved, even if the mass of the object is unknown. In the future these operations will probably be performed by a microprocessor because of the relatively sophisticated techniques involved, but the analog controller designed here should provide the microprocessor with the control interface necessary to generate the appropriate gripper response.

## VII. ACKNOWLEDGMENTS

The gripper mechanical design was initially conceived by R. A. Boie. He and M. S. Sibilia constructed the gripper from this design. The linear position sensor is due to G. L. Miller. W. J. Kropfl designed and programmed the computer interface. The robot and gripper systems are now running under an executive called NRTX developed by D. A. Kapilow. Without their efforts the gripper could not have come to life.

## REFERENCES

1. J. L. Nevins and D. E. Whitney, "Computer Controlled Assembly," Sci. Amer., *236*, No. 2 (February 1978), pp. 62–74.
2. M. R. Cutkowsky, "Position Sensing Wrists for Industrial Manipulators," Carnegie Mellon Tech. Rep. CMU-RI-TR-82-9, July 1982.
3. H. Hanafusa and H. Asada, "Stable Prehension of Objects by a Robot Hand with Elastic Fingers," Proc. 7th Int. Symp. Ind. Robots, Tokyo, October 1977, pp. 361–68.
4. M. K. Brown, "Computer Simulation of Controlled Impedance Robot Hand," IEEE Int. Conf. Robotics, Atlanta, GA, March 1984, pp. 442–50.
5. G. L. Miller, private communication.
6. C. T. Chen, *Introduction to Linear System Theory*, New York: Holt, Rinehart, and Winston, 1970.
7. D. A. Kapilow, unpublished work.
8. N. Hogan, Outlook for the Implementation of Robot Technology Symp., M.I.T. Industrial Liaison Program, February 1983.
9. B. Carnahan, H. A. Luther, and J. O. Wilkes, *Applied Numerical Methods*, New York: Wiley, 1969.
10. L. Collatz, *The Numerical Treatment of Differential Equations*, third ed., Berlin: Springer-Verlag, 1960.

## APPENDIX A

### *Runge-Kutta Method for the Solution of Differential Equations*

Runge-Kutta methods for solving general differential equations are well known and probably the most widely used algorithms for this purpose. The particular algorithm employed in this study is a fourth-order formula with coefficients attributed to Kutta (see Ref. 9). The algorithm solves the basic first-order equation:

$$\dot{x}(t) = f(x, t) \tag{30}$$

for $x(t)$, where $t$ is the independent variable. Since any high-order

differential equation can be written as a set of first-order differential equations, an equation of arbitrary order may be solved by repetitive application of the first-order algorithm.

Equation (1) is integrated over a small interval $h$ of the independent variable, which is termed the integration interval or step size. Each interval starts at an initial condition (e.g., $x(0)$) and concludes at an estimated value for $x(t)$ at the end of the interval, [e.g., $x(h)$], which provides the initial conditions for the next integration interval. This process is repeated, yielding $x(kh)$ for $k = 1, 2, \cdots, n$. For systems of first-order differential equations, the integration is applied to each equation in parallel for each step.

The fourth-order integration formula used is

$$\hat{x}(t + h) = \hat{x}(t) + h(k_1 + 2k_2 + 2k_3 + k_4)/6 \tag{31}$$

$$k_1 = f(x, t) \tag{32}$$

$$k_2 = f(x + hk_1/2, t + h/2) \tag{33}$$

$$k_3 = f(x + hk_2/2, t + h/2) \tag{34}$$

$$k_4 = f(x + hk_3, t + h). \tag{35}$$

Four evaluations of $f(x, t)$ are required for each integration step. This formula reduces to Simpson's rule if $f(x, t)$ is a function of $t$ only.

The integration truncation error committed at each integration interval is dependent upon the size of the interval $h$ and for an $m$th-order Runge-Kutta method the error is, in general, $O(h^{m+1})$. The actual error committed is further dependent in a complicated manner upon the dynamics of the equation. More specifically, a smaller interval will be required to maintain the same error bounds during rapidly varying periods of the solution function $x(t)$ than will be required when the solution function is slowly varying. Since $f(x, t)$ must be evaluated four times for each integration interval and $f(x, t)$ may be quite complicated and computationally expensive, it is desirable to keep $h$ as large as possible without incurring excessive error accumulation. For this reason the integration interval is adaptively increased and decreased as the integration proceeds.

To determine the proper integration interval during the integration process, an estimate of the truncation error being committed at each step is necessary. Several methods for estimating truncation error and adjusting step size have been reported in the literature (e.g., Collatz[10]); however, these methods are often nearly as time-consuming as the integration itself or suffer from certain serious failure modes. The Collatz method, for example, is only a qualitative measure, which is quite efficient, but suffers from a divide-by-zero problem when the slope of $x(t)$ becomes zero. A new method employed in this implemen-

tation of the algorithm was developed by the author to avoid excessive computation and eliminate the possibility of failure due to special cases of the solution. This method is also a qualitative measure and does not give a very accurate estimate of the true truncation error, but empirical study indicates it does yield a figure of merit that is within about an order of magnitude of the true error. By specifying figure-of-merit bounds that are an order of magnitude smaller than the maximum error required, we can easily maintain a sufficiently small integration interval without excessive computation or other complications.

This error estimator is based on a measure of the difference in truncation error expected between a second-order Runge-Kutta method and the fourth-order Runge-Kutta. Equation (35) is a second-order predictor for the solution at the end of the integration interval, $x(t + h)$. Recall that the truncation error committed at each step by an $m$th-order integration is $O(h^{m+1})$. By comparing $k_4$ to the solution obtained from the fourth-order integration and scaling the result by $h^2$, an error estimate proportional to the fourth-order truncation error is obtained. That is,

$$\text{error} = \alpha(h^2)\,|\,k_4 - \hat{x}(t + h)\,|, \tag{36}$$

where $\hat{x}(t + h)$ is the fourth-order solution for $f(x, t)$, $h$ is the integration interval, and $\alpha$ is a constant (usually between 0.1 and 10). If the error estimate exceeds a predetermined bound, then the integration interval is reduced to one-half its current value. Likewise, if the error estimate is more than (say) a thousand times less than the error bound, then the interval is increased to twice its previous value.

## APPENDIX B

### *State Equation for the Two-Fingered Gripper*

The following listing is written in the C programming language. It describes the complete state equation for the two-fingered gripper with common-mode feedback and the electrical time constants.

```
int gripper (t, y, dy)
double t, y[], dy[];
{
  double u1(), u2();
  double fabs(), log10();
  double kg, pg, f, f1;
/* state variables for the robot gripper:

  0. left finger position
  1. left finger velocity
  2. left motor angle
```

```
 3. left motor angular velocity
 4. right finger position
 5. right finger velocity
 6. right motor angle
 7. right motor angular velocity
 8. rubber ball position
 9. rubber ball velocity
10. left vel. RC network
11. left acc. RC network
12. right vel. RC network
13. right acc. RC network
14. common-mode vel. RC network
15. common-mode acc. RC network
16. left motor driver RC
17. right motor driver RC
*/
  kg = 4.16e6; /* spring constant and damping coefficient
    for gears */
  pg = 322.32;
/* compute state derivative function for left hand finger
  system */
  dy[0] = y[1];
  if(fabs((f = rg * y[2] - y[0])) > H){  /*gear force */
    f1 = (f > 0. ? (f-H) : (f+H)) * kg + (rg * y[3] - y[1]) *
      pg;
    if(f > 0.){
      f1 = (f1 > 0. ? f1 : 0.);
    }else{
      f1 = (f1 < 0. ? f1 : 0.);
    }
  }else{
       f1 = 0.;
  }
  if((if = y[0] - y[8] + R) > 0.){  /* rubber ball force */
    f2 = (f *k3 + (y[1] - y[9]) * p3);
    f2 = (f2 > 0. ? fs : 0.);
  }else{
    f2 = 0.;
  }
  dy[1] = (-P * y[1] + f1 - f2)/M;
/* compute left motor current and voltage */
    Ia1 = y[16];
    if(fabs(Ia1) > Imax){
      Ia1 =(Ia1 > 0. ? Imax : -Imax);
```

```
    }
  V1 = Ra * Ia1 + La * (Ia1 - Ia1sv)/dt + Ka * y[3];
  if(fabs(V1) > Vmax){
    V1 = (V1 > 0. ? Vmax : -Vmax);
    Ia1 = (V1 + La * Ia1sv/dt - Ka * y[3]/(Ra + La/dt);
  }
  dy[2] = y[3];
  dy[3] = (Km * Ia1 - p * y[3] - f1 * rg)/m;  /*torque */
/* compute state derivative for right hand finger system */
  dy[4] = y[5]
  if (fabs ((f = rg * y[6] - y[4])) > H){  /* gear force */
    f1 = (f > 0. ? (f - H) : (f + H)) * kg + (rg * y[7] - y[5]) *
      pg;
    if (f > 0.){
      f1 = (f1 > 0. ? f1 : 0.);
    }else{
      f1 = (f1 < 0. ? f1 : 0.);
    }
  }else{
    f1 = 0.;
  }
  if ((f = y[8] + R - y[4]) > 0.){  /*rubber ball force */
    f3 = f * k3 + (y[9] - y[5]) * p3;
    f3 = (f3 > 0. ? f3 : 0.);
  }else{
    f3 = 0.;
  }
  dy[5] = (-P * y[5] + f1 + f3)/M;
/* compute right motor current and voltage */
    Ia2 = y[17];
    if(fabs(Ia2) > Imax){
      Ia2 = (Ia2 > 0. ? Imax : -Imax);
    }
  V2 = Ra * Ia2 + La * (Ia2 - Ia2sv)/dt + Ka * y[7];
  if(fabs(V2) > Vmax){
    V2 = (V2 > 0. ? Vmax : -Vmax);
    Ia2 = (V2 + La * Ia2sv/dt - Ka * y[7]/(Ra + La/dt);
  }
  dy[6] = y[7];
  dy[7] = (Km * Ia2 - p * y[7] - f1 * rg)/m;
/* compute state derivative for rubber ball */
  dy[8] = y[9];
  dy[9] = (f2 - f3)/m3;
/* state equations for electronic circuitry */
```

```
    dy[10] = (y[0] - y[10])/RC;
    dy[11] = (dy[10] - y[11]/RC;
    dy[12] = (y[4] - y[12])/RC;
    dy[13] = (dy[12] - y[13])/RC;
    dy[14] = ((y[0] + y[4]) - y[14])/RC;
    dy[15] = (dy[14] - y[15])/RC;
    dy[16] = (-a * dy[11] - b * dy[10] + (c + f) * (u1(t) - y[0])
      - d * dy[15] - e * dy[14] + f * (u2(t) - y[4]) - y[16])/
      1.2e - 4;
    dy[17] = (-a * dy[13] - b * dy[12] + (c + f) * (u2(t) - y
      [4]) - d * dy[15] - e * dy[14] + f * (u1(t) - y[0]) -
      y[17])/1.2e - 4;
    return (18);
}
```

## AUTHOR

**Michael K. Brown,** B.S., 1973, M.S., 1977, and Ph.D., 1981 (Electrical Engineering), University of Michigan, Ann Arbor; Burroughs Corporation, 1973–1980; AT&T Bell Laboratories, 1980—. From 1973 to 1976 Mr. Brown was employed with the Burroughs Corporation and was involved in the development of ink jet printer systems. From 1976 to 1980 he continued his work with Burroughs as a consultant while pursuing his Ph.D. degree at the University of Michigan. His thesis was in the area of image processing and pattern recognition. In 1980 he joined the Speech Processing Group at AT&T Bell Laboratories, where he was involved in research in speech recognition and synthesis techniques. Since 1983, he has been with the Robotics Principles Research Department.